

Supporting Information

A 3D-Printed Microfluidic Gradient Generator with Integrated Photonic Silicon Sensors for Rapid Antimicrobial Susceptibility Testing

Christopher Heuer^{†,a,c}, John-Alexander Preuss^{†,a,b}, Marc Buttkewitz^a, Thomas Scheper^a, Ester Segal^c and Janina Bahnemann^{a,b}

S1. 3D Printing: Orientation and Repeatability

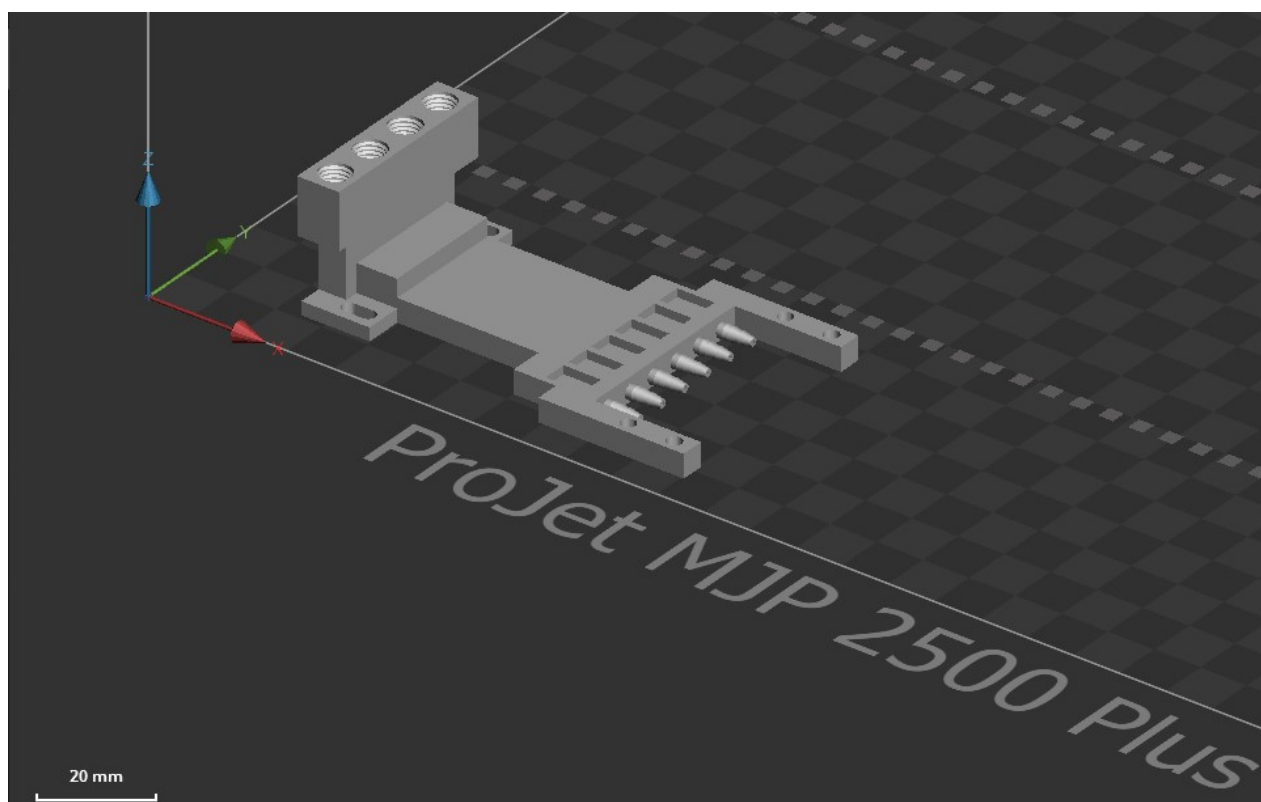


Figure S1. Orientation of the 3D model in the printing software "3D sprint". The large flat bottom surface is oriented towards the printing platform, and the inlets are facing upwards.

The printing accuracy was determined as follows: 3D models with open channels of different heights (300 μm , 500 μm , and 750 μm) were designed and 3D-printed in different directions (x, y, z). Using a digital microscope (VHX-6000, Keyence GmbH, Neu-Isenburg, Germany), height profiles were recorded using the options “depth composition” and “profile” (100x magnification). The channel height was determined as the height difference between the top and the bottom of the structure.

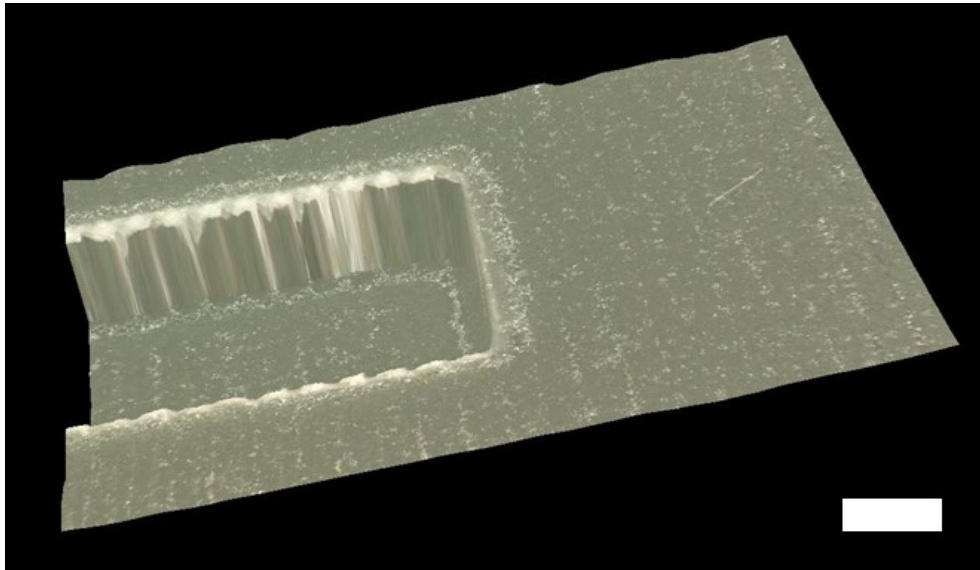


Figure S2. 3D visualization of the 3D-printed open channel with a designed height of 500 μm recorded by digital microscopy. The scale bar indicates 500 μm .

Table S1. Design vs. measured heights for different printing orientations (standard deviation for n=3).

Design (μm)	X (μm)	Y (μm)	Z (μm)
300	305 \pm 10	314 \pm 8	282 \pm 1
500	489 \pm 13	499 \pm 9	475 \pm 3
750	729 \pm 11	750 \pm 11	720 \pm 4

S2. Fabrication of Microwell Photonic Silicon Chips

1. 4-inch silicon wafers (Siltronic, France) with a SiO₂ layer (hard mask) of ~1000 Å thickness were used for the fabrication of the microwell photonic silicon chips.
2. Vaporized hexamethyldisilazane (HMDS) acting as an adhesion promoter was applied to the wafer before a positive photoresist AZ1512 was applied, and the wafer was baked at 110 °C for 90 s. All processes were performed using an automatic coater (Delta 80 Rc, SUSS Microtec, Germany).
3. Laser writing using a laser lithography system (DWL 66+, Heidelberg Instruments, Germany) was used to pattern the desired microstructure for the following etching procedures.
4. Tetramethylammonium hydroxide (TMAH) 10 % as developer reagent was added to the wafer dissolve residual photoresist using an automatic developer (Delta 8+, SUSS Microtec, Germany).
5. Reactive ion etching (Plasma-Therm Etching System 790, Plasma-Therm LLC, USA) was used to open the hard mask (SiO₂) at the designated positions before deep reactive ion etching (Plasma Etcher Versaline, Plasma-Therm LLC, USA) was applied to etch the microwell structure into the silicon substrate.
6. Residual photoresist and hard mask were removed from the areas that were not exposed to light and etched. For this purpose, the wafer was treated with 1-Methyl-2-pyrrolidone (NMP) for 25 min at 70 °C, MLO 07 for 15 min at 70 °C, piranha solution (H₂SO₄:H₂O₂ = 2:1), and buffer oxide etchant (BOE) for 5 min.
7. RCA cleaning of the wafer was performed. For this purpose, the wafer was treated with piranha solution (H₂SO₄:H₂O₂ = 2:1) for 10 min, diluted HF solution HF(49%):H₂O (1:50) for 10 s and NH₄OH(30%):H₂O₂(30%):H₂O (1:1:4) at 75 °C.
8. The resulting wafers were coated again with photoresist to protect their microstructure during the dicing procedure into 5 × 5 mm chips using an automated dicing saw (DAD3350, Disco, Japan).
9. The photonic silicon chips were washed with acetone to remove the photoresist and oxidized for 1 h at 800 °C in a furnace (Lindberg/Blue M 1200 °C Split-Hinge, Thermo Scientific, USA).

S3. Gradient Generator Design and Principle

For a gradient generator with n outlets, each outlet Out_i is supposed to carry the same volume flow. Thus, for incoming inflows Q_A and Q_B with relative concentrations of $c_A = 1$ and $c_B = 0$, respectively, the total flow rate C is

$$C = Q_A + Q_B \quad (1)$$

Accordingly, the total flow rate of each outlet i is

$$\frac{1}{n}C = Q_{A_i} + Q_{B_i} \quad (2)$$

With

$$\sum_{i=1}^n Q_{A_i} = Q_A \quad (3)$$

$$\sum_{i=1}^n Q_{B_i} = Q_B \quad (4)$$

Each concentration can be described as a mixing ratio a to b . For instance, a concentration of 0.25 requires a mixing ratio $a = 1$ and $b = 3$. Since the mixing ratio of a mixing level i is

$$\frac{Q_{A_i}}{Q_{B_i}} = \frac{a}{b} \quad (5)$$

Regarding equation (2), the sum of two flow rates needs to result in $\frac{1}{n}C$. We define $P_{i,A}$ as the fraction from A on the mixture at outlet i and $P_{i,B}$ vice versa.

$$\frac{P_{i,A}}{n(P_{i,A} + P_{i,B})}C + \frac{P_{i,B}}{n(P_{i,A} + P_{i,B})}C = \frac{1}{n}C \quad (6)$$

The sum of all fractions is calculated as

$$P_A = \sum_{i=1}^n \frac{P_{i,A}}{n(P_{i,A} + P_{i,B})} \quad (7)$$

$$P_B = \sum_{i=1}^n \frac{P_{i,B}}{n(P_{i,A} + P_{i,B})} \quad (8)$$

The second flow rate Q_B can be calculated for a given flowrate Q_A as

$$Q_B = \frac{P_B}{P_A} \cdot Q_A \quad (9)$$

The mixing channels of each level i are parallelized resistances/ lengths. Therefore, the length of each side of a level is inversely proportional to the fraction of each flow rate.

$$L_{i,A} = \frac{1}{\frac{P_{i,A}}{n(P_{i,A} + P_{i,B})}} \quad (10)$$

$$L_{i,B} = \frac{1}{\frac{P_{i,B}}{n(P_{i,A} + P_{i,B})}} \quad (11)$$

For clarity, the length of each channel can be normalized to the first channel of a side

$$L_{i,A}^{norm} = \frac{L_{1,A}}{L_{i,A}} \quad (12)$$

$$L_{i,B}^{norm} = \frac{L_{1,A}}{L_{i,B}} \quad (13)$$

The resulting parameters for a six-outlet, two-fold dilutions series gradient generator are summarized in Table S1. For a total flow rate of $1000 \mu\text{L min}^{-1}$ Q_A and Q_B are 323 and $677.3 \mu\text{L in}^{-1}$, respectively, as $\frac{P_B}{P_A}$ is approximately 2.096.

Table S2: Summary of mixing ratio parameters a and b as well as resulting relative lengths for an exponential (two-fold dilution series) gradient generator.

Mixing level i	Relative concentration	a	b	$L_{i,A}^{norm}$	$L_{i,B}^{norm}$
1	1	1	/	1	/
2	0.5	1	1	2	2
3	0.25	1	3	4	1.333
4	0.125	1	7	8	1.143
5	0.0625	1	15	16	1.066
6	0	/	1	/	1

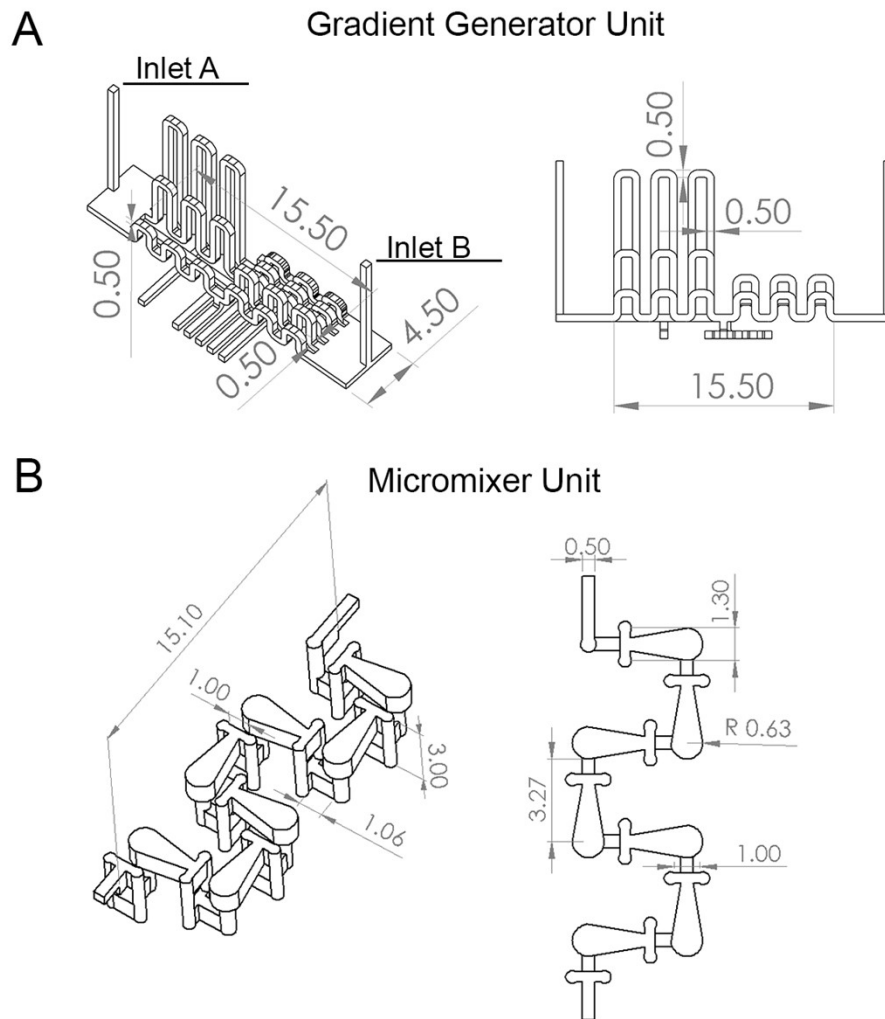


Figure S3. Detailed technical drawings of (A) the gradient generator unit and (B) the micromixer unit of the microfluidic gradient generator device. All dimensions (grey) are stated in mm.

S4. Gradient Generator Characterization

To study the impact of micromixers on the gradient accuracy and concentration homogeneity at each outlet, we performed CFD simulations with and without integrated HC-micromixers. As depicted in Figure S1, the results indicate that the averaged concentration is the same with and without micromixer integration. However, for on-chip measurements, we recommend micromixer integration since high inhomogeneities appear in outlets numbers 2-5 at the chosen flow rate of $1000 \mu\text{L min}^{-1}$ when no micromixers are integrated.

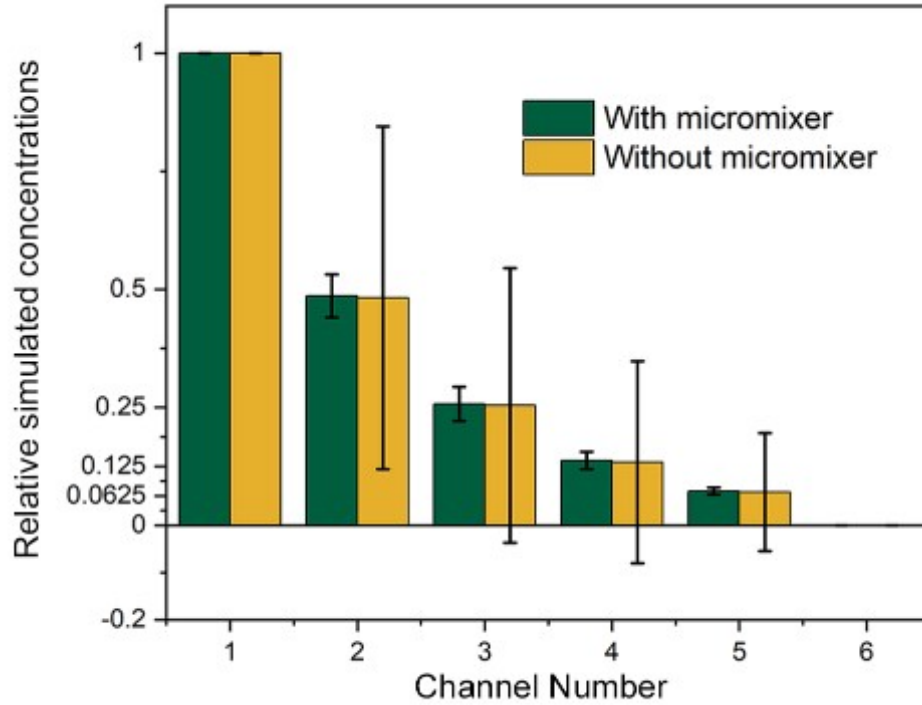


Figure S4. Impact of HC-micromixers on gradient accuracy and concentration homogeneity at each outlet. CFD simulations at a total flow rate of $1000 \mu\text{L min}^{-1}$ were used to determine the concentration at each outlet with and without integrated micromixers. Error bars indicate the standard deviation of the concentration distribution at each outlet. Low standard deviations indicate high homogeneity, while high standard deviations indicate low homogeneity.

For experimental flow rate determination, deionized water was introduced at a total flow rate of $\sim 1000 \mu\text{L min}^{-1}$ ($677.3 \mu\text{L min}^{-1} + 323 \mu\text{L min}^{-1}$) and collected from every outlet for 1 min and weighted using an analytical balance (BCE 224I-1S, Sartorius AG, Göttingen, Germany). The flow rate was determined using 1 g mL^{-1} as the density of water.

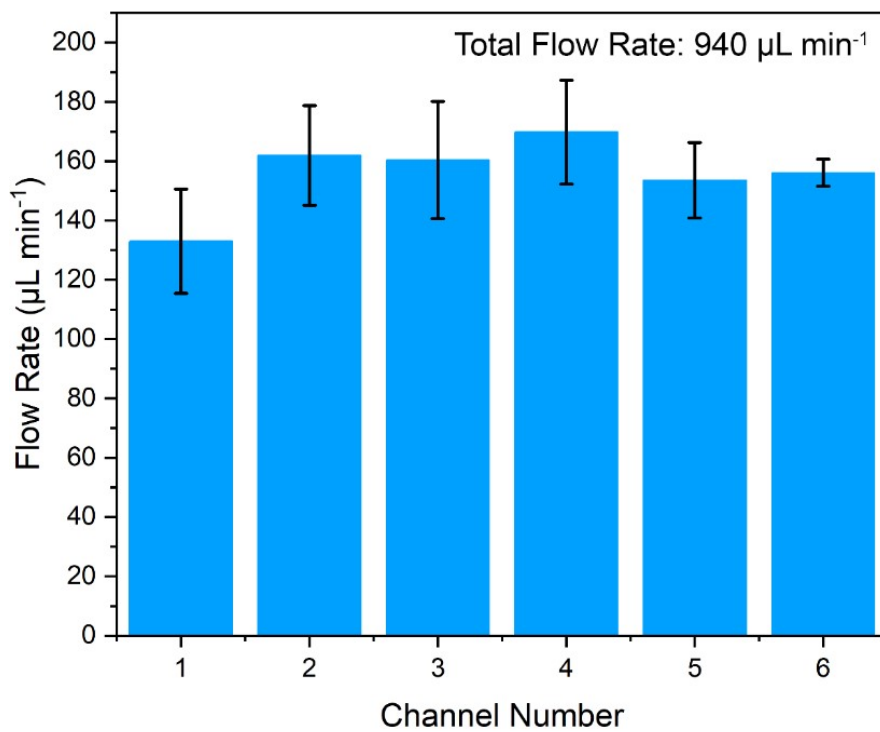


Figure S5. Experimental evaluation of flow rates at each outlet. Error bars indicate the standard deviation of three experiments. The total flow rate of $940 \mu\text{L min}^{-1}$ is consistent with the initial flow rate of $1000 \mu\text{L min}^{-1}$. The slight discrepancy may be explained because the fluids cannot be continuously collected from the outlets as they emerge only drop by drop.

S5. GG-enabled BMD results

Table S3 Summary and comparison of MIC values obtained by GG-enabled BMD, manual reference BMD, and MIC values published by EUCAST.

Pathogen - Drug Combination	GG-enabled BMD. (MIC)	Reference BMD (MIC)	EUCAST Data (MIC) ^{c)}
<i>S. marcescens</i> vs. ciprofloxacin	0.0625 mg L^{-1}	$0.0625 \text{ mg L}^{-1 \text{ a)}$	$0.008 - 0.25 \text{ mg L}^{-1 \text{ [1]}}$
<i>E. coli</i> vs. gentamicin	0.125 mg L^{-1}	$0.125 \text{ mg L}^{-1 \text{ a)}$	$0.008 - 2 \text{ mg L}^{-1 \text{ [1]}}$
<i>C. auris</i> vs. voriconazole	0.016 mg L^{-1}	$0.016 \text{ mg L}^{-1} - 0.03 \text{ mg L}^{-1 \text{ b)}$	$0.008 - 4 \text{ mg L}^{-1 \text{ [2]}}$

^{a)} Three BMD tests, each with $n \geq 3$ wells for every concentration tested; ^{b)} five BMD assays, each with $n \geq 3$ wells for every concentration tested; ^{c)} MIC range for susceptible wild-type bacteria and entire range for *C. auris*.

S6. GG-enabled PRISM assay

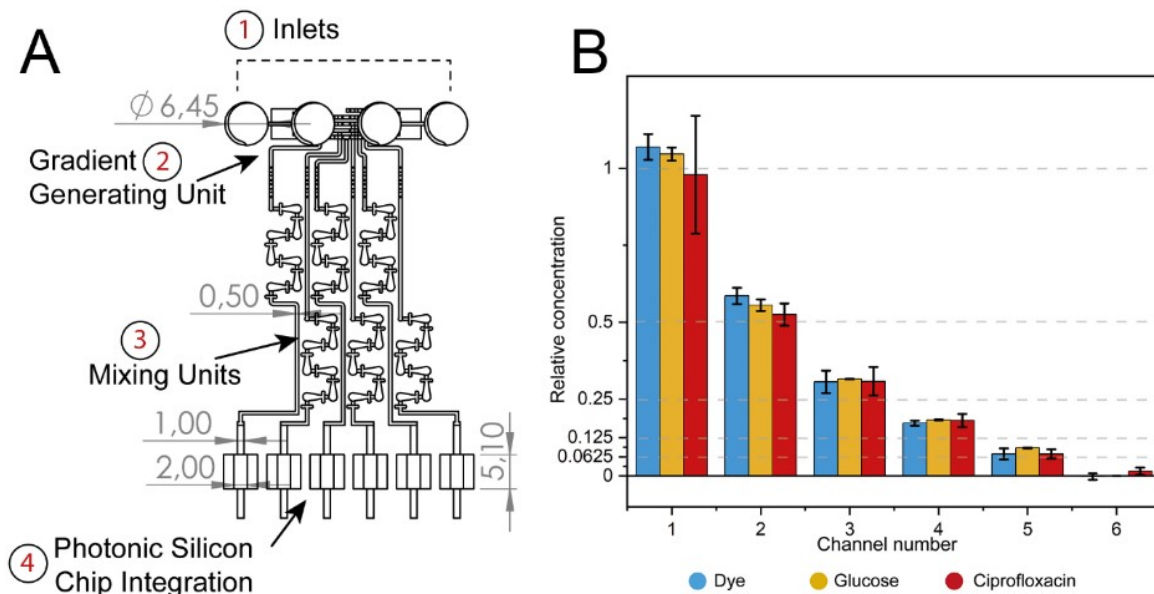


Figure S6. Microfluidic GG device for photonic silicon chip integration. (A) Technical drawing of the GG that has been modified for photonic silicon chip integration. The individual integration of the chips (size 5 x 5 mm) is enabled by six square-shaped chambers (size 5.1 x 5.1 mm) that are open to their bottom. (B) Importantly the chip integration does not impair the gradient generating accuracy as accurate gradients with high coefficients of determination (R^2) of 0.9966 (dye), 0.9967 (glucose), and 0.9941 (ciprofloxacin) are obtained. All calibration curves were accurate with $R^2 \geq 0.999$.

In the GG-based PRISM assay, suspensions of *E. coli* (McFarland 0.5) and 1 mg L⁻¹ ciprofloxacin (source fluid) and *E. coli* (McFarland 0.5) without antibiotic (sink fluid) are introduced for 5 min into the GG-device before the bacteria are given 10 minutes to settle within the microstructure, and the optical assay (PRISM) is initiated. To confirm that such an experimental procedure in which the bacteria are exposed to the highest tested ciprofloxacin concentration for 5 minutes before being diluted to the designated antibiotic concentrations does not cause flawed MIC values, a standard BMD with *E. coli* (McFarland 0.5) and ciprofloxacin (Figure S4A) and a modified BMD (Figure S4B) for this pathogen drug combination were performed. In the modified BMD, *E. coli* (McFarland 0.5) is incubated at 1 mg L⁻¹ ciprofloxacin for 5 minutes before a two-fold dilution series is performed in cell suspensions at the same cell density to reach the designated antibiotic concentrations. As demonstrated in Figure S4, for both procedures, the same MIC value is obtained.

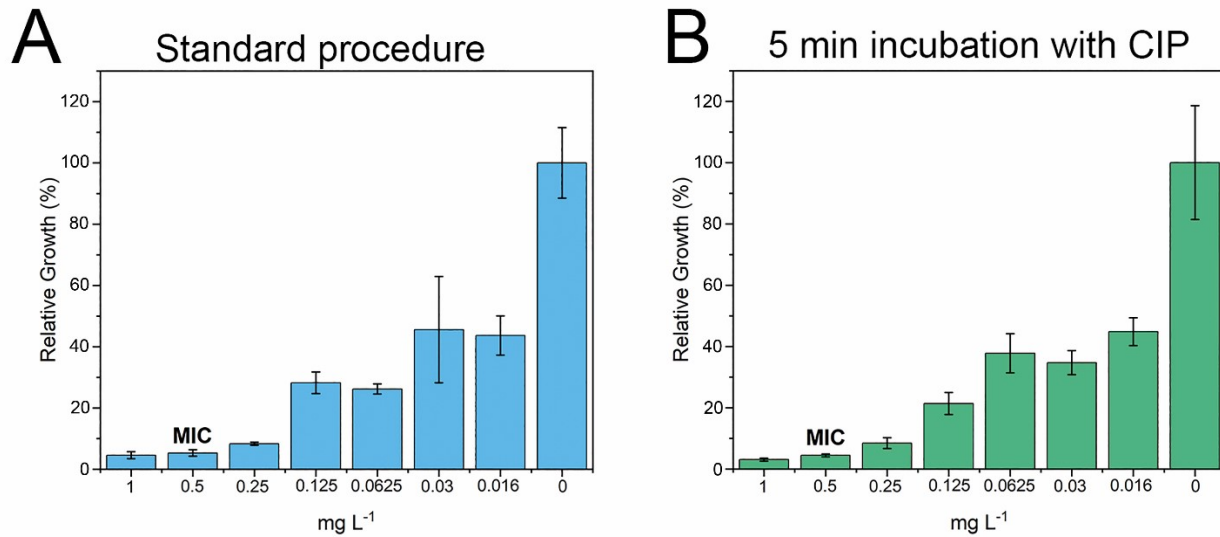


Figure S7. Comparison of BMD results for *E. coli* (McFarland 0.5) and ciprofloxacin (CIP) for (A) a standard procedure and (B) a modified BMD in which the bacteria are exposed for 5 minutes to the highest tested antibiotic concentration (CIP: 1 mg L⁻¹) before being diluted to the designated antibiotic concentrations. The MIC was defined as the lowest antibiotic concentration at which no growth was visible.

A typical clinical workflow consists of pathogen isolation from the patient and identification which precede the AST step.^{3,4} Thus, culturing remains a prerequisite for AST and typically the inoculum for AST is prepared from microbial cultures grown on agar plates overnight and standardized to a cell density corresponding to the McFarland 0.5 standard, see Table S4. Thus, our assay and the use of McFarland 0.5 is tailored to the clinical workflow and highly suitable for application in clinical settings.

Table S4. Comparison of the GG-based PRISM assay to gold standard BMD and commercialized clinically relevant AST methods.

Method	Principle	Sample Matrix	Test Matrix	Cell Density Standardization	Inoculum	Time
GG-based PRISM	Refractive index changes within a silicon diffraction grating	Colonies from fresh agar medium	Microstructured photonic silicon sensors in liquid growth medium	McFarland 0.5 (10 ⁸ cells mL ⁻¹)	McFarland 0.5	90 min
Gold Standard BMD ^{5,6}	Visual or spectrophotometric observation of turbidity	Colonies from fresh agar medium	Liquid growth medium	McFarland 0.5	5 x 10 ⁵ cells mL ⁻¹	18 h
State-of-the-Art Vitek 2 ^{7,8}	Automated turbidity measurements	Colonies from fresh agar medium	Liquid growth medium	McFarland 0.5	~10 ⁷ cells mL ⁻¹	8 h
Agar-based Etest ^{9,10}	Zone of inhibition around a strip with an antifungal gradient	Colonies from fresh agar medium	Agar plate	McFarland 0.5	McFarland 0.5	16 - 20 h

References

- 1 European Committee on Antimicrobial Susceptibility Testing, EUCAST Antimicrobial wild type distributions of microorganisms, <https://mic.eucast.org/>, (accessed: June 20, 2022).
- 2 M. C. Arendrup, A. Prakash, J. Meletiadis, C. Sharma, A. Chowdhary, *Antimicrob. Agents Chemother.*, 2017, **61**, e00485-17.
- 3 C. Heuer, J. Bahnemann, T. Scheper and E. Segal, *Small Methods*, 2021, **5**, 2100713
- 4 H. Leonard, R. Colodner, S. Halachmi and E. Segal, *ACS Sens.*, 2018, **3**, 2202–2217.
- 5 EUCAST, EUCAST definitive document E.DEF 7.3.2 Method for the determination of broth dilution minimum inhibitory concentrations of antifungal agents for yeasts, https://www.eucast.org/fileadmin/src/media/PDFs/EUCAST_files/AFST/Files/EUCAST_E_Def_7.3.2_Yeast_testing_definitive_revised_2020.pdf, (accessed June 17, 2022).
- 6 International Organization for Standardization, ISO 20776-1:2020.
- 7 Ligozzi, C. Bernini, M. G. Bonora, M. de Fatima, J. Zuliani and R. Fontana, *J. Clin. Microbiol.*, 2002, **40**, 1681–1686.
- 8 bioMérieux, Vitek2 GN Card Instructions REF21341. Can be downloaded from the bioMérieux Resource Center after registration: <https://resourcecenter.biomerieux.com/search/>
- 9 bioMérieux, Etest Application Guide, https://www.biomerieux-usa.com/sites/subsidiary_us/files/supplementary_inserts_-_16273_-_b_-_en_-_eag_-_etest_application_guide-3.pdf, (accessed June 17, 2022).
- 10 bioMérieux, Etest Ciprofloxacin Instructions REF412311/423766. Can be downloaded from the bioMérieux Resource Center after registration: <https://resourcecenter.biomerieux.com/search/>